NUMERICAL ANALYSIS OF RAIL – STRUCTURE INTERACTION AND RESONANCE IN RAILWAY BRIDGES

Marco Petrangeli, Cristiano Tamagno
University of Pescara, Italy, INTEGRA, Italy

Abstract
The paper illustrates the results of a research carried out by the authors on the effects of rail structure interaction and resonance. The study makes use of the recent insertion of a finite element for modelling the ballast response into the finite element code FIBRE. The element complies with the Italian railway specifications and has been tested and validated according to a standardized procedure based on three blind numerical tests defined by the Italian Railway agency. Since the program is capable of carrying out step-by-step non-linear analyses in the time domain it can be now used for multiple type of analyses with the same finite element model (mesh). Using the program state-of-the-art library of fibre beam-column elements, ultimate limit state analyses can be performed under live load and seismic input. Rail-structure interaction can be analysed with the train running at low speed (quasi static). With the same trains running at higher speeds the resonant behaviour can then be assessed. In all type of analysis, the effect of the long welded rail can be taken into account as it significantly modify the response of small span bridges.

After discussing the new ballast finite element and the principal program features, a numerical case study is presented to illustrating all the different types of analyses that can be performed with the program. Making use of time histories and stress-strain histories of the different bridge elements, the principal mechanisms governing the response of railway girders and bridges are discussed. Finally, the effect of rail on the seismic response of these structures is investigated comparing the structural response with and without rails.

1. Introduction

Rail-structure interaction and resonance analyses are today required by the Italian Norms [1] for any bridge that doesn't fall within specified limits. These limits are basically maximum span length (30m circa for reinforced and prestressed concrete) and stiffness

This paper is part of the 7th International Conference on Short and Medium Span Bridges, Montreal, Canada, 2006.

of piers and foundations that must be particularly high and evenly distributed among the different supports. These limits are specifically addressed to minimize the risk of rail instabilities due to thermal and horizontal live load actions in the long welded rail since rail joints are generally forbidden.

When bridges fall within the specified limits, equivalent linear elastic analyses can be performed. Outside these bounds, non-linear step-by step analyses are required for the rail-structure interaction [2] and dynamic analyses for the resonance.

General purpose Finite Element (FE) program can often be used although not straightforwardly as both the load input and the ballast behaviour are hardly available in the specific form required. Awkwardness in the load input is the major cause of concern for the resonance analysis since a large spectrum of loading histories needs to be investigated. Ballast constitutive behaviour, vice versa, can be the problem in the interaction analysis since the specific constitutive behaviour may be difficult to obtain using the simplified non-linear models available.

2. The fibre finite element program

Fibre is a 3D non-linear FE program for the analysis of civil structures. The program has been developed in the last 15 years from the family of codes known as DRAIN3D and ANSR [3]. Developments have addressed different aspects of civil engineering, although major achievements were recorded in the field of non-linear response of framed structure [4][5]. The non-linear fibre element with fibre shear modelling available in the program [5] can be used for the post elastic analysis of bridges and other railway structures subjected to live and seismic load. Shear capabilities are particularly useful in railway engineer as squat piers are often encountered among these structures.

More generally, the need for non-linear analysis of structures has received a major acceleration by the introduction of the new European Norm [6][7] and more recently by the new “Displacement Based Approaches” [8][9].

It was therefore decided to upgrade the program with the necessary features to carry out the interaction and resonance analyses as well. It is now possible to perform with the same model and program all the above said types of analyses, including large displacement and buckling analysis as total Lagrange formulation is used.

3. The ballast constitutive behaviour

The Italian Railway Norm [1] define the ballast response under horizontal loading with a family of elasto-plastic force-displacement curves (Fig.1) with a constant yield displacement (Δ_y) of 2mm and a yield force (F_Y) linearly dependent on the axial load (N) as follows:

$$F_Y(N) = F_{min} + \Phi N \quad (1)$$

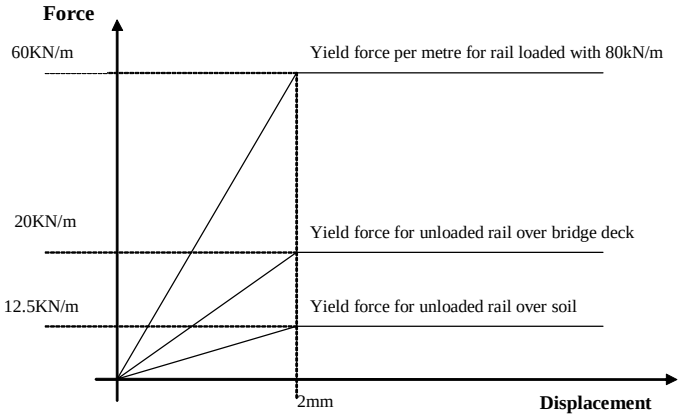

Figure 1: Ballast force-displacement curves

The friction coefficient Φ and the minimum friction force F_{min} being set to 0.5 and 20 kN/m on bridge deck and 0.59375 and 12.5 kN/m on soil, as shown in Fig. 1. The axial behaviour is assumed to be linear elastic with stiffness equal to 130 MN/m/m. Other parameters which are not explicitly specified in the Norm have been assumed as follows:

- Unloading is linear-elastic, with the modulus a function of the axial load.
- Tangent modulus K(N) for loading, reloading and unloading branches is found with the following expression:

$$K(N) = F_Y(N)/\Delta_y \quad (2)$$

- The friction behaviour is fully 2D.

It should be remarked that the assumption made for the tangent modulus is one out of a number of other available options. As a matter of fact the variable stiffness found with (2) cannot be obtained by putting in series a linear-elastic element with a friction element. Also noteworthy is that while axial force influences the shear yielding force, the shear response does not influences the axial one. This is a gross approximation as generally granular materials show a very strong dilatancy when subject to shear actions. Nonetheless, the vertical behaviour of the ballast-rail system has negligible effect on the bridge response as the load applied to the rail (train loading) is largely independent of the vertical response of it.

4. The ballast finite element

The ballast finite element is a purely shear type element with 2 nodes and 6 DOF. The vector of nodal displacement being:

$$U^e = (U^i_x, U^i_y\ U^i_z\ U^j_x\ U^j_y\ U^j_z)^T \quad (3)$$

The element uses a displacement approach where the element generalised deformation $\varepsilon^e = (\Delta_x\ \Delta_y\ \Delta_z)^T$ (the axial elongation and the two generalized distortions perpendicular to the element axis) are found multiplying the vector of nodal displacements by the compatibility matrix D:

$$\varepsilon^e = D\ U^e \quad (4)$$

Once deformations are computed, the generalised stresses $\sigma^e = (N\ T_y\ T_z)$ are found with the above mentioned constitutive behaviour that has fully cyclic capabilities. The possibility of a tension cut-off in the ballast axial response is also available to modelling rail buckling. Once the stresses are known, the nodal forces $F^e = (F^i_x, F^i_y\ F^i_z\ F^j_x\ F^j_y\ F^j_z)^T$ are found using the transposed of D. Since the element disregards equilibrium it is necessary to keep is length negligible with respect to the other structural dimensions.

5. Moving load generation

Both interaction and resonance analyses require a number of different trains to be generated and applied over the structures. For the interaction analysis, the Italian Norms requires the same trains used in static analysis such as the standard LM71, SW/0 and SW/2. For the resonance analysis 5 different trains are to be used instead. Each of them is to be applied over a range of velocities up to the specified maximum that varies from 200 to 350 km/h at 10 km/h increment. Given the large amount of loading histories to be generated, the program was enriched with automatic generation capabilities. These capabilities allow for the description of any generic train as an unlimited series of point and distributed loads.

6. A case study

The proposed case study refers to the large prefabricated box girder used along the new railway line Turin-Milan [10]. The girder has a net span of 32.1m and weights over 400ton alone. Joining together 2 of these girders a deck or 13.6m width and 34.5m gross span is obtained. Over 250 of these girders are found along the above said line.

Although this type of beam has been used for long viaducts, the proposed case study refers, for the sake of simplicity and clarity, to a single span. Sub-structures are supposed to have an horizontal stiffness of 100 MN/m/m which roughly correspond to that of a short abutment/pier.
Other geometric and mechanical characteristics being the following: rail area = 76.9 cm^2, rail inertia = 3055 cm^4, ballast thickness = 0.35 m, distance between box girder and rail axis = 1.68 m, distance between box girder axis and support = 4.22 m, box girder inertia vertical inertia = 5.95 m^4, self weight and permanent load 7500 kN.

6.1 The finite element model

The analyses have been performed for half deck (a single box-girder) with a 2D model (Fig.2). By doing this, minor transverse and torsional effects are neglected

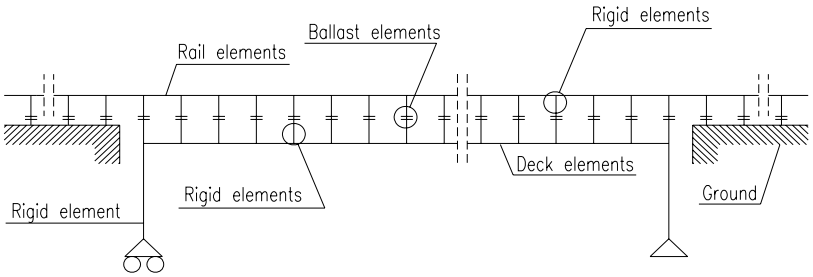

Figure 2: Overview of the of the 2D FE model

In the interaction analysis it is fundamental to place each element in its exact vertical position. The deck elements have been therefore placed along the deck axis and so it has been done for the rail. Rigid links connect the deck axis to the supports. Rigid links in series with ballast elements connect the deck to the rail. Further details on the deck rail connections are to be found in the next sub-chapter.

Except for the ballast, linear elastic behaviour has been assumed for all the other elements. According to the Italian Norms, the rail has been extended for 100m in both directions beyond the bridge assuming the line runs on embankment (ballast on ground). Total length of the model is therefore 234.5m; the abscissa starts on the left. The sliding support, on the left, is therefore placed at abscissa x=100m, the fixed support, on the right, at abscissa x=133.3m. Node spacing for the deck and rail has been set equal to the sleeper spacing, which is 0.6m. This is generally not necessary since it may be computationally demanding and therefore a larger spacing is generally advisable although requires some scaling to be carried out properly, as explained in the following paragraph.

6.2 Modelling of deck-rail connection

The connection between the bridge deck and the rail is made of three components; the rail-sleeper joint, the sleeper itself and the ballast. As far as the shear behaviour is concerned, the response is governed by the ballast since the other two elements can be considered completely rigid. When it comes to bending, neither the rail-sleeper joint nor the sleeper-ballast connections are rigid compared to the rail flexural inertia.

The model should therefore account for the flexural compliance of these connections since axial load in the rail causes bending moment in these elements. The authors have investigated both a pin and a built in connection as shown in Figure 3. The real situation is somewhat intermediate between the two, with higher rotational stiffness when the

sleepers are loaded by the train and cannot tilt.

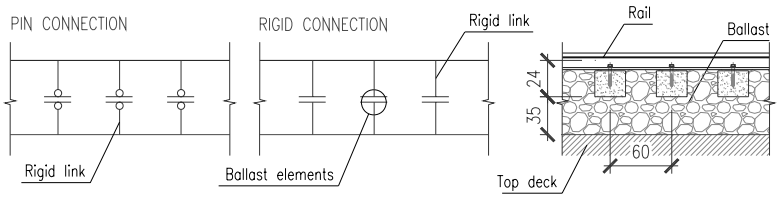

Figure 3: Modelling of deck-rail connection

When a fixed connection is used, results show that the point of contra flexure tends to occur very closely to the rail and thus the rail is not subjected to significant bending. When, vice versa, a pin connection is used, bending moment will arise in the rail equal to the product of the shear force carried by the ballast times the rail-pin distance. Since it makes sense to place the pin near the sleeper intrados, the eccentricity of the axial load carried by the rail is 20-25cm circa. Consequently, if the deck rail connection has a longitudinal spacing (d) larger then that of the sleepers (0.6m circa), it is necessary to scale the rail bending stiffness (inertia). The rail equivalent inertia (I_{eq}) to be used in the model is found with the following relation:

$$I_{eq} = I_{rail} * (d / 0.6)^2 \quad (5)$$

6.3 The applied loadings

The analysis has been carried out by initially applying a uniform temperature increase to the deck of $\Delta T = 15^oC$ and subsequently letting the train (LM71) run over the whole rail length. Although with a single rail alignment, the model can still take two different trains running in opposite direction as generally required by the Italian Norm; again, for the sake of simplicity, a single accelerating train has been applied.

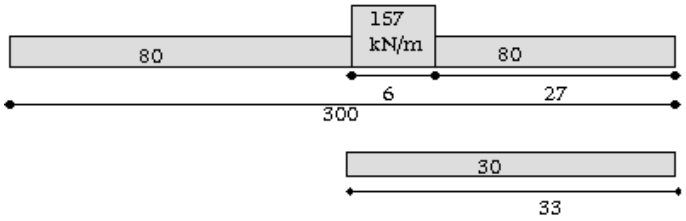

Figure 4: The LM71 loading scheme

The 300m long train, starts at abscissa x=0 and terminates when the trailing cars are out of the model that means the total running length is 534.5m. For the resonance analyses, the first of the 5 different trains specified by the Italian Norm has been used. This is made of 12 ALE601 cars running at up to 200 km/h at 10km/h interval.

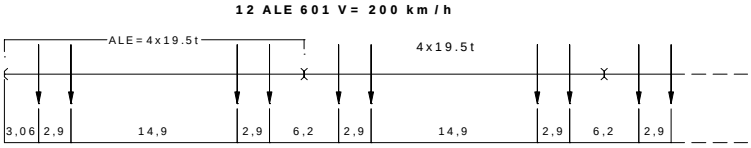

Figure 5: The ALE train for the resonance analysis

7. The rail-structure interaction

The most intuitive effect of rail structure interaction is found in the horizontal force of the fixed support. With deck temperature changes, the rail pushes against the fixed support (Fig.6). For a typical 32m span as the one under consideration, the force tend to an asymptote which is attained when the ballast yields along the whole deck length (F=12.5x32.1 = 400KN

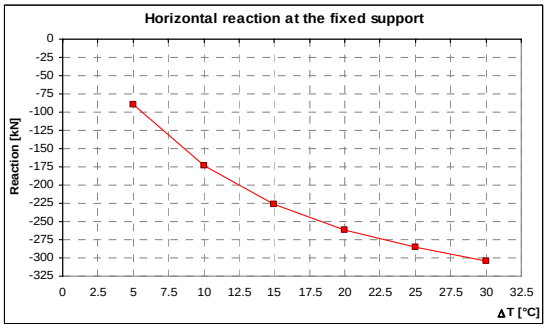

Figure 6: Fixed support horizontal reaction

The next figures show the force (Fig.7) and displacement (Fig.8) distribution along the rail for the 15^{o} temperature change required by the norms. Maximum compression is found at the sliding support (deck expansion joint) with σ_c=-8.8Mpa. Maximum tensile stress few metres ahead of the fixed support (on the deck) with σ_t=6.8Mpa.

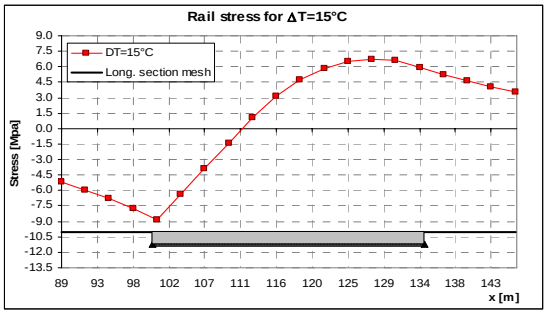

Figure 7: Rail stresses due to temperature.

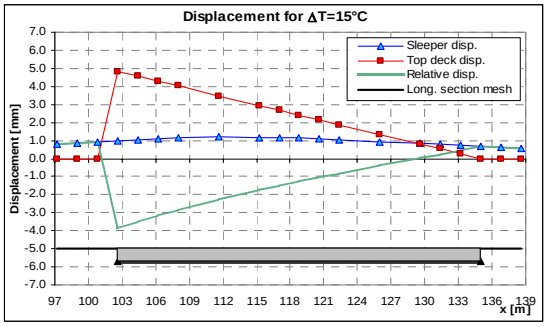

Figure 8: Rail displacement due to temperature

The Time Histories (THs) of the fixed support horizontal reaction due to the combined effect of temperature and train acceleration, as well as train only, are plotted in Figure 9 as a function of the abscissa x of the train. The maximum reaction is attained just before the train start to leave the deck at abscissa 134m.

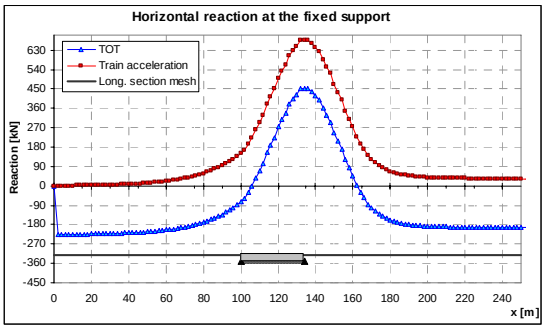

Figure 9: Horizontal reaction TH

The TH of the rail stress above the sliding support is plotted in Figure 10. The accelerating train pull the rail until it reach the deck when it start to push it adding this effect to the temperature one until the maximum value of σ_c=-15.2 Mpa is found with the train starting to leave the deck (abscissa x= 134 m). The corresponding stress TH over the fixed support is plotted in Figure 11.

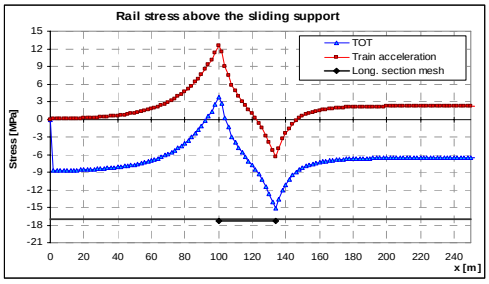

Figure 10: Rail stress THs at expansion joint

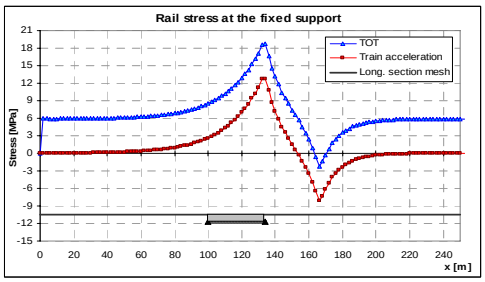

Figure 11: Rail stress THs at fixed support

The rail displacement TH with respect to the ground at the sliding support (x=100m) are plotted in Figure 12. The figure shows the rail is displaced backwards by both temperature and the approach of the accelerating cars up to a maximum of 2.6mm.

It is interesting to note that the rail remain displaced after the train hasrun over the deck because of the permanent plastic deformation in the ballast. This residual displacement is the cause for the residual tension in the rail of the previous two figures.

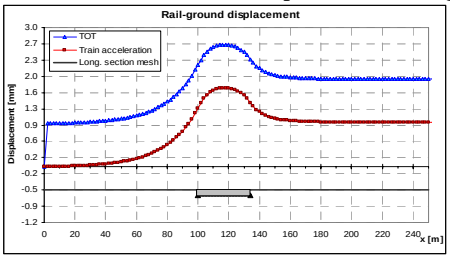

Figure 12: Rail displacement THs

Finally the displacement of the rail and deck at the instant of maximum relative displacement (x=118m) due to train only is plotted in Fig. 13. The displacement of the deck is that due to vertical bending. That of the rail is due to the accelerating force of the front cars.

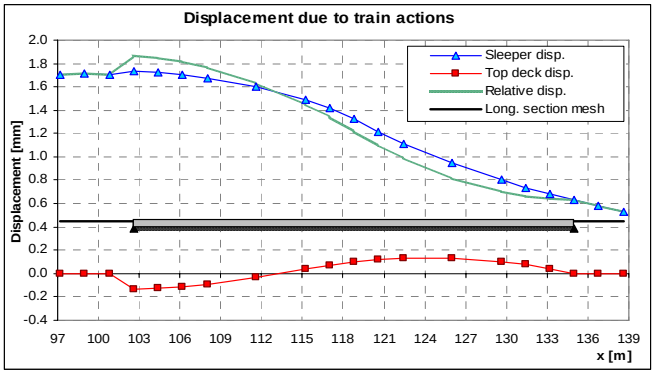

Figure 13: Rail and deck displacements at the instant of maximum relative displacement

8. The resonance analysis

The same single box girder has been subjected to the ALE601 train passing at increasing speed up to 200km/h. The real structure would in effect couple bending and torsion with a single train running over it. Since the first torsional frequency (f_T=9.86Hz) is more than 1.5 higher the corresponding bending one (f_V=4.61Hz), Italian Norm allows the use of a plane (2D) model ignoring the torsional effects. For each sampled speed the Dynamic amplification factor is plotted (Fig.14) as the ratio of the maximum dynamic deflection over the corresponding static deflection. Three curves are plotted, the response of the structure with and without tracks and the response of the structure without tracks and with a simplified input where the coupled axes (2.9m apart) have been merged in one.

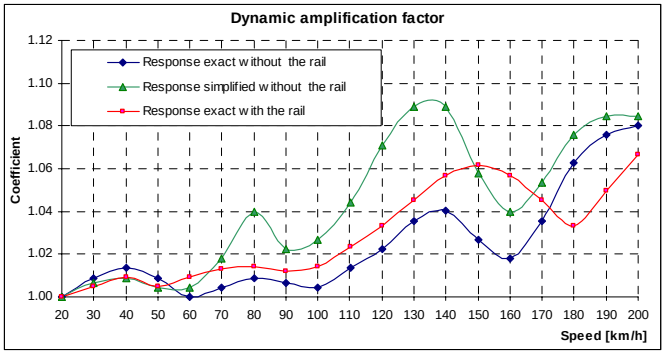

Figure 14: Dynamic amplification factor

The figure shows how the amplification factor for the girder under consideration is modest. This is due to the weight of the structure (7500kN) and to the very disperse frequency contents of the train itself. The load axels spacing varies in fact, from 2.9 to 18m circa. By merging the adjacent axes one can see how the amplification factor increases significantly. Taking into consideration the rail, the bridge frequencies increases and the same shift towards higher speeds in found for the amplification factor.

9. The seismic response with and without rail

Given the rail axial stiffness and the hysteretic behaviour of the ballast a significant reduction of the bridge response under seismic input is expected when the long welded rail is properly taken into consideration. Obviously, some bridge configurations under sever seismic input may cause the rail buckling and therefore a strong reduction in the dissipating capacity of the ballast. This aspect is being addressed in a separate research by the same authors.

In the present work, an EC8 compatible, medium intensity accelerogram has been generated with a Peak Ground Acceleration of 0.25g. The structure with and without track has been subjected to this ground motion applied in the longitudinal direction (parallel to the rail axis). In order to amplify the bridge response, the stiffness of the fixed support has been reduced by a factor of 4 and 20 with respect to the previous tests.

The long welded rail reduces the response (displacement of the fixed support) by 60% and 73% respectively (Fig.15). These results are obtained for a maximum force in the rail which is well below the buckling critical value as shown in Figure 16. Maximum forces are also comparable for the 2 stiffness since a complete yielding of the ballast is attained in both cases.

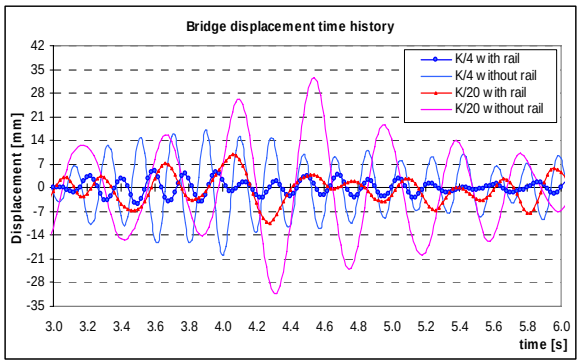

Figure 15: Bridge displacement THs

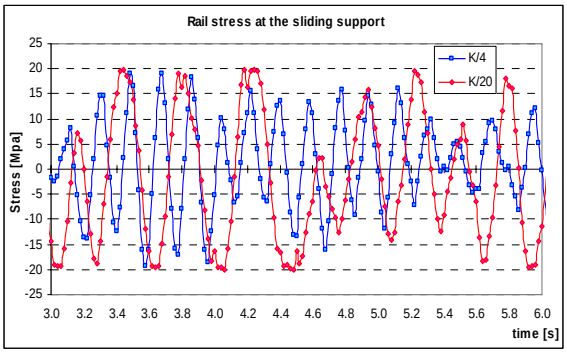

Figure 16: Rail stress THs at the sliding support

Finally, the hysteretic force-displacement response of a ballast element near the expansion joint (sliding support) is plotted (Fig.17). The yielding force is equal to 7.5kN which is the maximum force transmissible by a single ballast element spaced at 0.6m (12.5kN/m * 0.6m = 7.5kN).

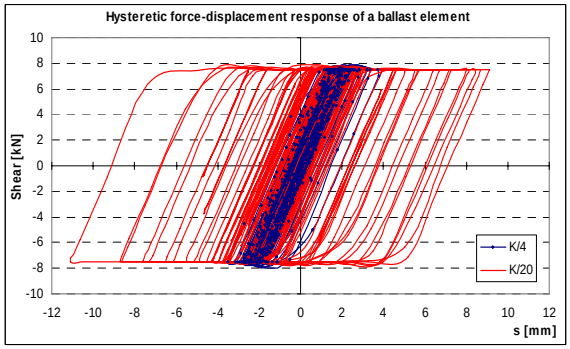

Figure 17: Ballast Force-Displacement response

10. Conclusion

Rail expansion joints are hardly used along the Italian network and their use discouraged because of maintenance requirements. Especially when it comes to bridges, these are designed so as to avoid the necessity of rail joints.

This approach is one of the reasons for the extended use of simply supported beams with limited length between adjacent deck expansion joints. It also discourage the realization of high performance continuous or cable supported structures or slender and more appealing sub-structures unless reliable numerical simulations can be performed to asses the forces that may arise into the rails.

These forces are caused mostly by temperature effect and seismic loading, where applicable, but also live loading and breaking/ accelerating can be of certain relevance.

Because all these phenomena are highly non-linear a single numerical tool to deal with all of them is required as stress superposition is generally not applicable. Once a reliable tool is available, the application of the long welded rail can be possibly extended to longer bridges as the stresses in the rail are easily controlled and the rail itself may have some positive effect on the bridge structural behaviour.

On the other hand, generalization of the above phenomena is hardly possible as the actual force distribution depends on so many geometrical and mechanical parameters that generalization is hardly possible and a specific analysis of the structure unavoidable.

11. References

1. Istruzione F.S. N.I/SC/PS-OM/2298 del 13-1-1997 – "Sovraccarichi per il calcolo dei ponti ferroviari. Istruzioni per la progettazione, l'esecuzione e il collaudo".
2. A. Conti Puorger (1992). "La triade treno-binario-struttura problematiche specifiche della interazione", Ingegneria Ferroviaria, Settembre 1992.
3. D.P.Mondkar, G.H.Powell (1975). "Static and dynamic analysis of nonlinear structures". University of California, Berkely. Report No. UCB/EERC-75/10.
4. Petrangeli, M. and Ciampi, V. (1996). "Equilibrium based numerical solutions for the nonlinear beam problem", Int. Journal for Num. Meth. in Engrg, 40(3), 423-438.
5. Petrangeli, M., Pinto, P.E. and Ciampi, V. (1999). "A Fibre Element for cyclic bending and shear. Part I and II, J. Engrg. Mech., ASCE, 125(9).
6. CEN EUROCODE 2, "Design of Concrete Structures", UNI-ENV-1992 – 1
7. CEN EUROCODE 8 "Design Provisions for Earthquake Resistance of Structures" ENV 1998-2: Bridges. Brussels.
8. BSSc, NEHRP guidelines for the seismic rehabilitation of buildings, FEMA-273, developed by ATC for FEMA, Washington, D.C., 1997
9. SEAOC, Vision 2000, Performance based seismic engineering of buildings, Structural Engineers Association of California, Sacramento, 1995
10. Petrangeli M., Andreocci C., Magorfi F., Orlandini M. Geremia G. (2006). "Large Concrete Precast Box Girders along the New Italian High Speed Railway", 7th Int. Conf. on Short & Medium Span Bridges, IABSE, Monreal Aug. 23-25, 2006.